Artificial Neural Network for Improving the Motion Control Quality of Underwater Remotely Operated Vehicle

Umjetna neuronska mreža za poboljšanje kvalitete upravljanja kretanjem podvodne daljinski upravljane ronilice

Xuan-Kien Dang
Ho Chi Minh City University of Transport
AIT Research Group
Vietnam
E-mail: kien.dang@ut.edu.vn

Žarko Koboević
University of Dubrovnik
Faculty of Maritime Studies
Croatia
E-mail: zarko.koboevic@unidu.hr

Nguyen-Hoang Long Phan
Ho Chi Minh City University of Transport
AIT Research Group
Vietnam
E-mail: hoanglong5x9@gmail.com

Viet-Dung Do*
Ho Chi Minh City University of Transport
AIT Research Group
Vietnam
E-mail: dungdv@ut.edu.vn

Soi Ly
a) Ho Chi Minh City University of Transport
AIT Research Group, Vietnam
b) Dong An Polytechnic, Binh Duong, Vietnam
E-mail: lysoi@dongan.edu.vn

DOI 10.17818/NM/2025/2.1
UDK 621.398:629.584
004.032.26
Original scientific paper / *Izvorni znanstveni rad*
Paper received / *Rukopis primljen:* 21. 3. 2025.
Paper accepted / *Rukopis prihvaćen:* 3. 6. 2025.

Abstract

The Remotely Operated Vehicle (ROV) plays a crucial role in underwater surveys but faces challenges in complex environments with unmeasured variables, leading to inefficiencies in navigation. This paper develops a motion control solution for ROVs that utilizes Artificial Neural Networks (ANNs) to enhance control quality in response to environmental impacts. Firstly, the authors develop an Adaptive Fuzzy Control (AFC) to control ROV movements under varying environmental conditions, allowing for the collection of operational datasets. Next, the ROV motion controller is designed based on the ANN architecture to enhance control quality. Finally, experimental scenarios using MATLAB demonstrated that ANNs markedly improve control accuracy and overall performance for ROVs when following predetermined trajectories. This emphasizes their substantial potential in advancing autonomous marine applications.

Sažetak

Daljinski upravljana ronilica (engl. Remotedly Operated Vehicle – ROV) ima važnu ulogu u podvodnim istraživanjima, ali se suočava s izazovima u složenim okruženjima s neizmjerljivim varijablama, što dovodi do neučinkovitosti u navigaciji. U ovom se radu razvija rješenje za upravljanje kretanjem ROV-a koje se koristi umjetnim neuronskim mrežama (engl. Artificial Neural Networks – ANN) kako bi se poboljšala kvaliteta upravljanja kao odgovor na utjecaj iz okoliša. Autori razvijaju neizrazito adaptivno upravljanje (engl. Adaptive Fuzzy Control – AFC) za kontrolu gibanja ROV-a u promjenjivim okolišnim uvjetima, što omogućuje prikupljanje operativnih skupova podataka. Regulator za kretanje ROV-a dizajniran je na temelju umjetne neuronske mreže (engl. ANN) kako bi se poboljšala kvaliteta upravljanja. Konačno, eksperimentalni scenariji provedeni u MATLAB-u pokazali su da umjetne neuronske mreže značajno poboljšavaju točnost upravljanja, kao i ukupne performanse ROV-a pri praćenju unaprijed zadanih putanja. To naglašava njihov značajan potencijal u unaprjeđenju autonomnih pomorskih aplikacija.

KEY WORDS

Adaptive fuzzy control
artificial neural network
environmental disturbance
path planning
remotely operated vehicle

KLJUČNE RIJEČI

neizrazito adaptivno upravljanje
umjetna neuronska mreža
poremećaji okoliša
planiranje puta
daljinski upravljana ronilica

1. INTRODUCTION / *Uvod*

In the maritime industry, geological exploration and mapping of the ocean floor are necessary for helping sailors plan accurate routes to avoid collisions with underwater obstacles such as reefs. Significant oil and gas reserves are also located on the ocean floor, making geological inspections for exploration and exploitation essential. However, these exploration efforts face numerous challenges, as reserves are often situated beneath the ocean's surface. Technological developments have outfitted marine vehicles with equipment that helps prevent operator errors, which can lead to maritime accidents, while also improving operational efficiency [1]. This depth necessitates using specialized equipment, such as ROVs, that can function effectively in harsh marine environments. Underwater operations are always affected by unmeasured factors [2], such as currents, tides, and obstacles. As a result, operating ROVs requires adhering to high standards to ensure stable operation and precise control. In particular, the motion control process must minimize the effects of environmental disturbances to keep ROVs stable and operate accurately in deep-sea conditions. The motion control of the ROVs involves several key factors that ensure high-efficiency operation in offshore environments. The studies have focused on maintaining ROV stability at a fixed speed [3] and at varying speeds while moving

* Corresponding author

along a specified path [4]. These operations are influenced by various nonlinear factors and disturbances. Maintaining the correct direction while following the desired path is crucial to keep the ROV motion precise [5]. Further, the modern technique used to maintain direction while hovering [6], along with efforts to reduce energy consumption [7], is essential for the ROV's effective operation in actual conditions [8]. When the ROV reaches its working position, the dynamic positioning mode is activated to perform specific tasks. Concurrently, reducing the transmission delay of control signals from the mother ship is explored [9]. Besides, some studies have been conducted on achieving desired tilting motions to maintain balance and fuel economy [10] and adjust the tilt angle along the path according to specific mission requirements [11]. Therefore, the control algorithm is the most crucial factor, as it allows the ROV to adapt to nonlinearities and environmental disturbances.

Modern approaches to marine vehicle motion control have employed traditional control methods, notably Proportional-Integral-Derivative (PID) controllers [12-13], combined with advanced intelligent techniques to navigate predefined paths and maintain precise positional stability [14-15]. Nonetheless, a significant gap exists in the literature concerning the influence of actual environmental conditions on operational efficacy. To enhance navigational precision, sophisticated methods have been incorporated into the motion control framework. Fuzzy logic techniques are commonly utilized to dynamically tune controller parameters [16-17], while structural parameter optimization is frequently executed through particle swarm optimization algorithms, thereby improving the fidelity of operational signals [18-19]. The ant colony optimization has also demonstrated effectiveness in generating robust control parameters that facilitate collision avoidance in complex operations [20].

Artificial Intelligence (AI) has emerged as a crucial trend across various sectors due to its remarkable adaptability and flexibility. Its application in ROV control has led to significant advancements. AI-based control methods gradually supersede traditional algorithms, as they can adapt to diverse situations, process vast amounts of data, and learn from experience. One widely discussed approach involves using adaptive neural networks that determine linear controller parameters, known as ANNFOPID [21], which help minimize disturbances and manage uncertainties, ultimately enhancing trajectory tracking for autonomous underwater vehicles. Furthermore, using ANNs to control ROVs via sensor signals with pulse outputs ensures stability even in varying current conditions [22]. To minimize the impact of nonlinear components, a minimal learning parameter (MLP) is used to approximate control signals in dynamic system modeling [23]. Convolutional Neural Networks (CNNs) assess ambient conditions for the ROVs, though their effectiveness is limited in low-light situations [24]. In motion control, evolutionary algorithms optimize Neural Network (NN) parameters to reduce computation time [25] and maintain stability during dynamic system failures [26]. Recurrent Neural Networks (RNNs) help reduce vibration amplitudes in ROV motion by monitoring uncertain states [27]. Additionally, the NNs can adaptively adjust controller parameters to environmental changes [28] and simplify complex data processing in underwater vehicles using a combination of unweighted NNs and fuzzy logic [29]. Quality-based controller datasets are essential for developing stable and adaptive control models for ROVs under varying operating conditions.

This study proposes an ANN approach to improve the quality of ROV motion control under environmental influences. The main contributions are summarized as follows: *i*) Developing an AFC controller with parameters adjusted to accommodate input error variations and reduce the impact of nonlinear components during ROV motion; *ii*) Building an ROV motion controller based on the ANN, trained from a dataset of ROV operations under the environmental influence applying the AFC controller; *iii*) Verifying the proposed solution to control ROV motion according to two scenarios under environmental impact to evaluate the effectiveness of the proposed solution.

This paper is organized as follows: Section II provides an overview of ROV modeling, including remarks that outline the stages and goals of the study. Section III details the establishment of the basic AFC solution as well as the proposed ANN solution for controlling ROV motion. Section IV presents the simulations and testing scenarios. Finally, Section V concludes the paper and discusses future directions for the study.

2. MATERIAL AND METHOD / *Materijal i metoda*

2.1. Remotely operated vehicle model / *Model daljinski upravljane ronilice (engl. ROV)*

The motion of underwater vehicles is analyzed in six degrees of freedom using two coordinate systems. One of these is the body-fixed frame *XYZ*, which is related to the submerged vehicle. The other is the Earth-fixed frame $X_0Y_0Z_0$, which describes the vehicle's motion concerning the Earth (as shown in Fig. 1). Based on these two primary reference frames, the kinematic equations of the ROV are defined as follows [30]:

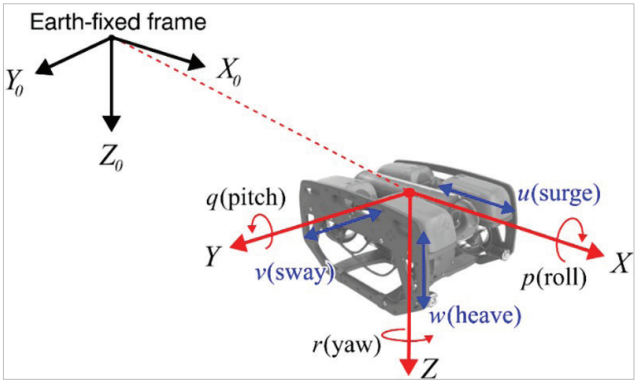

Figure 1 The coordinate system of the ROV motion
Slika 1. Koordinatni sustav kretanja ROV-a

$$\dot{\eta} = J(\eta)v \tag{1}$$

where η denotes the position and heading of the ROV within the Earth's coordinate system, while v represents the linear velocity along the body coordinate system of the ROV. The dynamic equation of the ROV is given by [31]

$$M\dot{v} + C(v)v + D(v)v + g(\eta) = \tau \tag{2}$$

in which M represents the total inertial mass of the ROV, including its augmented mass. C refers to the combined effects of the Coriolis force and the Centrifugal force generated by the actual weight of the ROV. Additionally, D signifies the damping component, which encompasses both linear and nonlinear elements. The variable g represents the vector of gravitational acceleration acting on the vehicle as it moves, while $\tau[\tau_x \tau_y \tau_z]$ denotes the vector that sums the forces and moments generated by the propulsion system and the rudder.

Remark 1: Environmental disturbances significantly affect the dynamics of ROV motion, introducing nonlinear factors that are challenging to quantify. As a result, the performance of the motion control system deteriorates.

In actual operations, the current is the main component affecting the ROVs during underwater missions. The impact of currents on the body alters the motion velocity, denoted as v. Therefore, it is assumed that the motion can be expressed using the relative velocity v_r [32] as follows:

$$v_r = v - \vartheta_c \tag{3}$$

The axial current velocity ϑ_c $[u_c, v_c, w_c]$ can be converted to $\vartheta_c^e[u_c^e, v_c^e, w_c^e]^T$, which is the current velocity along the Earth frame using the rotation matrix. The components of the vector ϑ_c^e are expressed as

$$\begin{aligned} u_c^e &= V_c \cos(\alpha_c)\cos(\beta_c) \\ v_c^e &= V_c \sin(\beta_c) \\ w_c^e &= V_c \sin(\alpha_c)\cos(\beta_c) \end{aligned} \tag{4}$$

whereas V_c represents the current velocity, α_c is the drift angle, and the slip angle β_c describes the direction of the current velocity.

Remark 2: Using conventional methods to control nonlinear ROV motion is inefficient. Additionally, as noted in Remark 1, the control deviation will increase significantly due to environmental disturbances.

2.2. Stages and goals / *Faze i ciljevi*

The AFC controller exhibits good response characteristics to nonlinear effects due to its capability to adapt to variations in input errors. However, the underwater environment introduces numerous error components that the basic solution does not handle effectively. To address this issue, it is essential to enhance the quality of control parameters using the ANN that has self-learning capabilities. The improvement aims to reduce random errors caused by the environment. Building an ROV control solution involves three main stages, as follows:

- *Stage 1* – Collecting the training dataset: The AFC controller is designed to control ROV motion by adjusting structural parameters to minimize input errors and reduce nonlinear effects. During operation, AFC controller values are compiled into a training dataset for the ANN algorithm, which improves quality and simplifies computations by eliminating fuzzy rules.
- *Stage 2* – Building the ANN controller: The ROV motion controller employs an ANN structure, as outlined in Algorithm 1. After training, the optimal neuron weights are integrated into the controller, enhancing its adaptability and response to environmental changes.
- *Stage 3* – Testing and evaluation: The proposed solution was tested in two scenarios simulating actual ROV operations: straight and short trajectory. The results were compared with other solutions based on quality assessment criteria, which highlighted its effectiveness.

3. MATERIAL AND METHOD / *Materijal i metoda*

3.1. Fuzzy Adaptive Control for ROV Motion / *Neizrazito adaptivno upravljanje za kretanje ROV-a*

This study introduces a fuzzy technique for adaptive tuning of basic PID controller parameters [33], referred as the AFC controller. This technique can adjust the parameters $K(K_{pf}, K_{if}, K_{df})$ in response to changes in the input error. The AFC control structure [34] for the adaptive tuning of the basic controller parameters is defined by

$$\tau_{AFC}(t) = K_{pf} e(t) + K_{if} \int_0^t e(t)dt + K_{df} \frac{de(t)}{dt} \tag{5}$$

The fuzzy model consists of a set of rules along with their corresponding results [35]. The If-Then rules are described as follows:

$$R_i: If\ \hat{x}_1\ is\ A_1^i \ldots and\ \hat{x}_n\ is\ A_n^i\ then\ k\ is\ B^i \tag{6}$$

with $A_1^i, A_2^i, \ldots A_n^i$ and B^i representing the fuzzy sets of input and output signals. This paper employs a fuzzy model based on Mamdani rules, utilizing the Max-Min inference rule and the Centroid defuzzification method. q represents the number of If-Then rules, and $\mu_{A_j^i}(\hat{x}_j)$ denote the Membership Functions (MFs). The outputs of the fuzzy model K are given by

$$K(\hat{x}) = \frac{\sum_{i=1}^{q} B^i \left[min_{j=1}^{n} \mu_{A_j^i}(\hat{x}_j) \right]}{\sum_{i=1}^{q} \left[min_{j=1}^{n} \mu_{A_j^i}(\hat{x}_j) \right]} \tag{7}$$

Let $\emptyset(\hat{x})=[\emptyset^1, \emptyset^2, \ldots, \emptyset^q]^T \in R^q$ represent a fuzzy basic vector [36] that is defined as

$$\emptyset(\hat{x}) = \frac{\left[min_{j=1}^{n} \mu_{A_j^i}(\hat{x}_j) \right]}{\sum_{i=1}^{h} \left[min_{j=1}^{n} \mu_{A_j^i}(\hat{x}_j) \right]} \tag{8}$$

The fuzzy sets are adjusted using the parameter vector δ^T, which corresponds to $B^i(i=1,2,\ldots q)$. The output of the fuzzy model is presented as linearized parameters as follows:

$$K(\hat{x}) = \delta^T \emptyset(\hat{x}) \tag{9}$$

The fuzzy model is based on the input reference value, the error e, and the error velocity de, to adjust the values of the three adaptation coefficients K_{pf}, K_{if} and K_{df}. The relationship between the input and output values is represented in 3D space, as illustrated in Fig. 2.

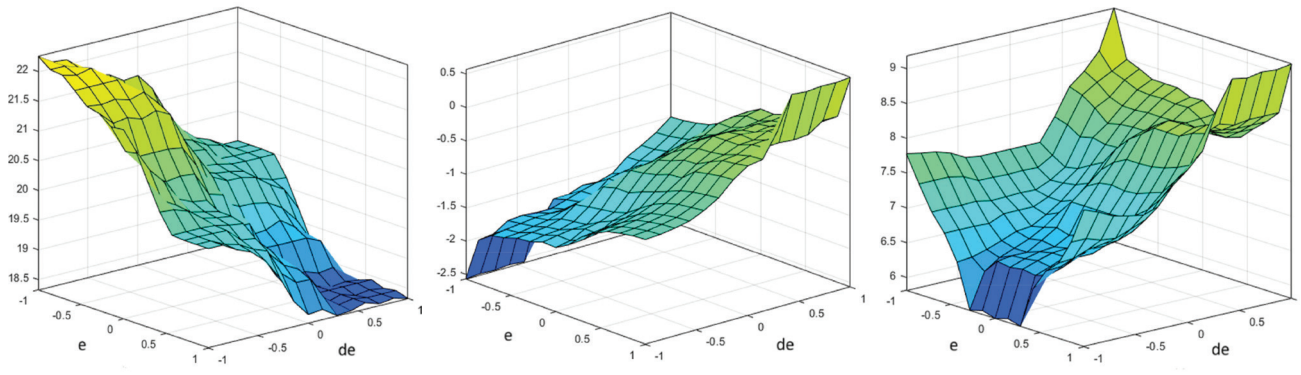

(a) (b) ((c)

Figure 2 Relationship between inputs e, de and outputs. (a) Output K_{pf}; (b) Output K_{if}; and (c) Output K_{df}

Slika 2. Odnos između ulaza e, de i izlaza. (a) Izlaz K_{pf}; (b) Izlaz K_{if}; i (c) Izlaz K_{df}

Fig. 2 illustrates how each fuzzy rule produces an output value based on changes in e and de. In the case of the output K_{pf} as shown in Fig. 2a, when both e and de are negative, K_{pf} increases to a positive value to correct the reduction in error. Conversely, K_{pf} decreases when e and de become positive. For the output K_{if}, depicted in Fig. 2b, the correction is also inversely proportional to the input error. However, the correction value for K_{if} is set much lower to prevent significant fluctuations. The response of K_{df}, shown in Fig. 2c, must be flexible to ensure system stability. Specifically, if the e and de values exceed acceptable thresholds (either too high or too low), K_{df} will increase sharply to respond to these rapid changes. Besides, as e and de approach zero, K_{df} tends to decrease slightly to help maintain system stability.

3.2. The ROV Motion Control for Using Artificial Neural Network / *Upravljanje kretanjem ROV-a korištenjem umjetnim neuronskim mrežama*

The AFC solution for controlling ROV motion is effective only with a defined range of flexible parameter adjustments. The influence of environmental conditions, as noted in Remarks 1 and 2, can result in significant discrepancies in control response. Fig. 3 provides an overview of the proposed solution to improve the motion control of the ROV. This paper proposes an ANN to enhance both the processing speed and accuracy of the ROV motion control, as described in Algorithm 1. The process of building an ROV motion controller using an ANN consists of four steps:

- *Step 1* - Building the NN structure: The feedforward architecture consists of three main components: the input layer, the hidden layers, and the output layer. The process for calculating the signals in the hidden layers using the nonlinear activation function is described in (11) and (12), whereas the determination of the network output is provided in (13). The input vector $in(t)$ is represented as

$$in(t) = \begin{bmatrix} e(t) \\ de/dt \\ \tau_{AFC}(t) \end{bmatrix} \quad (10)$$

The feedforward network is selected for its straightforward structure, linear computation from input to output, and state memory mechanisms found in more complex networks.

- *Step 2* - Training the control model: After establishing the NN structure, the control model carries out the training phase, updating the weights (ω) using the backpropagation algorithm in (16). The network's performance is assessed by applying the mean squared error loss function in (15), which measures the difference between predicted outputs and target values from the training data.
- *Step 3* - Optimizing the NN architecture: To improve performance and meet control system requirements, the model was experimented using NNs with 2 to 8 hidden layers, as indicated in setup Step 1, which involved varying the value of m in Algorithm 1. The goal was to assess how the depth of the network affects convergence and processing speed.
- *Step 4* - Extracting the control model: After determining the optimal NN structure and completing the training, the ROV control model is extracted, including its architecture, weights, and hyperparameters. The step ensures readiness for the next phase: deploying and testing the model in uncertain environments, as outlined in steps 15 and 16 of Algorithm 1.

In this study, we utilize Hyperbolic Tangent functions for the hidden layer and a linear activation function for the output layer to attain optimal performance. The output of the hidden layer [37-38] is defined by

$$h(z_j) = tanh(z_j) = \frac{2}{1 + e^{-2z_j}} - 1 \quad (11)$$

The output of the hidden layer is computed as follows [39-40]:

$$z_j = h(\omega_j \chi_i + \beta_j) \quad (12)$$

where ω_j represents the weight connecting neuron i in the input layer to neuron j in the hidden layer. Additionally, χ_i denotes the input for neuron i in the input layer. The notation β_j signifies the bias associated with neuron j in the hidden layer, which helps adjust the neuron's activation threshold and enhances its ability to learn complex patterns. Similarly, the input to neuron ℓ in the output layer is computed in the same way as described in (13).

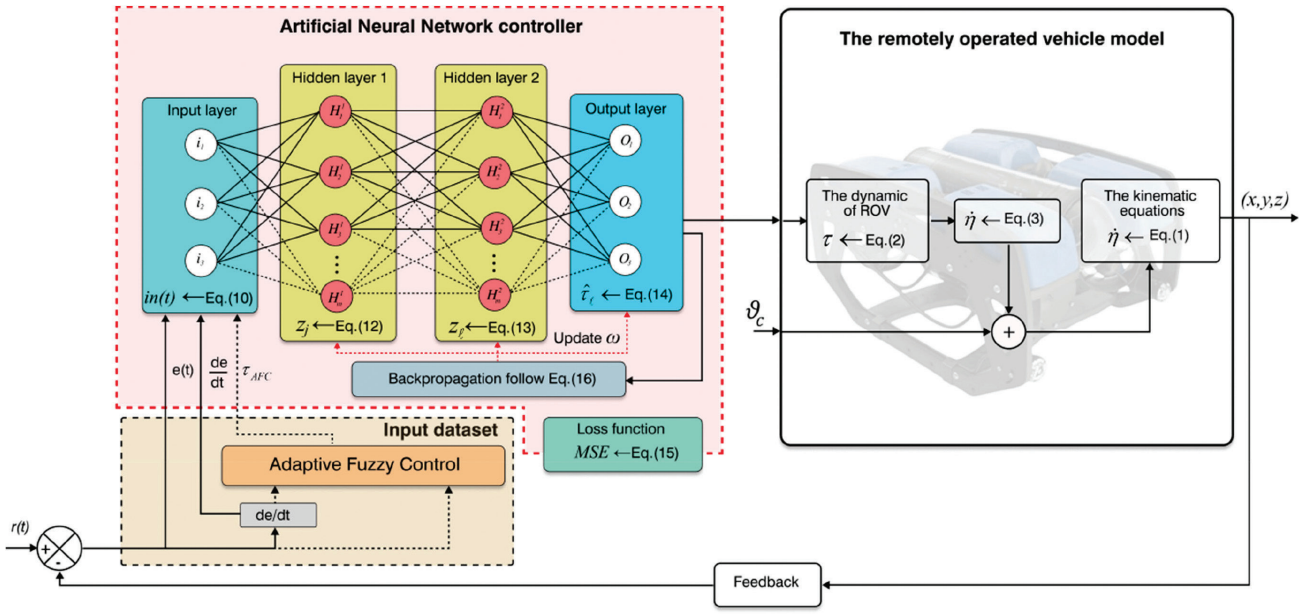

Figure 3 Overview diagram of the ROV control system utilizing an ANN controller
Slika 3. Pregledni dijagram sustava upravljanja ROV-om s ANN regulatorom

$$z_\ell = h(\omega_\ell z_j + \beta_\ell) \quad (13)$$

therein z_j is the activated output from the hidden layer *j*, while ω_ℓ determines its influence on the output neuron and the bias β_ℓ adjusts activation. Consequently, the $\hat{\tau}_\ell$ output value of the ANN is obtained through the linear activation function as [41]

$$\hat{\tau}_\ell = f(z_\ell) = [\hat{\tau}_x, \hat{\tau}_y, \hat{\tau}_z] \quad (14)$$

Several evaluation criteria exist for ANN models, including Root Mean Square Error of Approximation (RMSEA) [42] and Mean Square Error (MSE) [43]. In this study, we use the MSE function to assess the difference between the predicted output $\hat{\tau}_\ell$ and the desired output τ_ℓ as follows:

$$MSE = \frac{1}{N}\sum_{k=1}^{N}(\tau_\ell - \hat{\tau}_\ell)^2 \quad (15)$$

To optimize the learning performance of the ANN, this study utilizes the Levenberg-Marquardt training algorithm in conjunction with the Backpropagation technique [44]. This hybrid approach accelerates convergence by integrating the strengths of both Gradient Descent and Gauss-Newton methods, enhancing accuracy and expediting error minimization. The process for adjusting the weights using the Levenberg-Marquardt method [45] is outlined as

$$\omega(t+1) = \omega(t) - (Z^T Z + \lambda)^{-1} Z^T e(t) \quad (16)$$

in which, $\omega(t)$ denotes the weight vector at the t iteration with Z being the Jacobian matrix. Besides, $e(t)$ expresses the error at the t iteration, and λ is the adjustment parameter. Depending on the value of λ, the proposed ANN solution obtains different convergence values. If the value of λ is large, the ANN network converges slowly but stably. On the contrary, if the value of λ is small, the algorithm converges quickly but is prone to fluctuations.

Algorithm 1. Designing the ROV control model based on the ANN.	
	Input: datasets of $e(t)$, de/dt, and $\tau_{AFC}(t)$.
	Output: The ROV control model.
1	**Initialize** the training parameters: epoch←500, *learning rate*←0.000001, *hidden layer* ← *m*.
2	**Initialize** dataset 70% for training, 15% for testing, and 15% for validation.
3	**for** 0<*epoch*<500 **do**
4	**for** 1 < *hidden layer* < *m* **do**
5	Computing $z_j \leftarrow$ (12).
6	Computing $z_\ell \leftarrow$ (13).
7	Computing $\hat{\tau}_\ell \leftarrow$ (14).
8	If the termination condition is not satisfied, add *m* by 1 and repeat Step 4.
9	**end for**
10	Computing the loss function *MSE* ← (15).
11	Determining the weight adjustment ← (16).
12	Updating the weight function ω_j.
13	If the minimum loss value is not met, the *epoch* increases by 1 and returns to Step 3.
14	**end for**
15	Exporting the ROV control model.
16	Applying the control model to maneuver the ROV in test scenarios.
17	**end**

4. RESULTS AND EVALUATIONS / *Rezultati i vrednovanje*

4.1. Configuration Parameters / *Parametri konfiguracije*

The specifications for this study's ROV are based on the RRC ROV II model [46]. Table 1 presents the dynamic parameters relevant to the ROV's performance during aquatic maneuvers. To evaluate the efficacy of the proposed control strategies, the authors executed experiments encompassing both straight-line motion control (Scenario 1) and path-planning motion control (Scenario 2).

Table 1 The RRC ROV II parameters
Tablica 1. Parametri RRC ROV II

Parameters	Symbol	Value
ROV's Mass	m	115 (kg)
Gravitational force	W	1128.2 (N)
Added mass in X direction	$X_{\dot{u}}$	21.1403 (kg)
Added mass in Y direction	$Y_{\dot{v}}$	51.7 (kg)
Added mass in Z direction	$Z_{\dot{w}}$	92.451 (kg)
Linear damping force in X direction	X_u	253 (Ns²/m²)
Linear damping force in Ydirection	Y_v	1029.5 (Ns²/m²)
Linear damping force in Z direction	Z_w	1029.5 (Ns²/m²)
Nonlinear damping force in X direction	$X_{u\|u\|}$	423 (Ns²/m²)
Nonlinear damping force in Y direction	$Y_{v\|v\|}$	747 (Ns²/m²)
Nonlinear damping force in Z direction	$Z_{w\|w\|}$	735 (Ns²/m²)

Table 2 The tuning ranges of the AFC controller
Tablica 2. Rasponi parametara za podešavanje AFC regulatora

Motions	K_{pf}	K_{if}	K_{df}
Surge	[18, 30]	[-3.6, 1.2]	[6, 12]
Sway	[12, 18]	[-3.6, 1.2]	[18, 24]
Heave	[21, 28]	[-4.2, 1.4]	[21, 28]

The tuning ranges of the fuzzy functions for the AFC controller parameters are shown in Table 2. Thereby, adjusting the baseline parameters helps determine the optimal signal required to produce the output signal, which will serve as the training data set for the ANN.

Table 3 The ANN training parameters
Tablica 3. Parametri treniranja ANN-a

Parameter	Value
Epoch	500
Total node in hidden layer 1	32
Total node in hidden layer 2	16
Learning rate	0.000001
Loss function	MSE
Training Ratio	70%
Validate Ratio	15%
Testing Ratio	15%

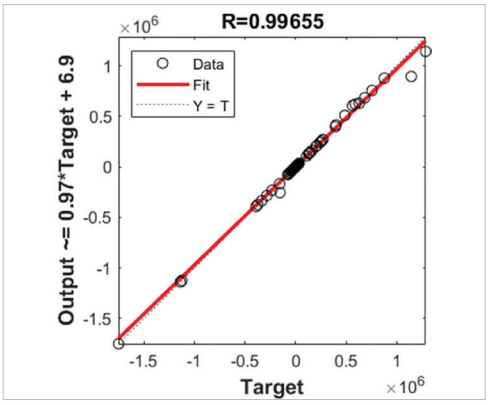

Figure 4 Result of the ANN model training
Slika 4. Rezultat treniranja ANN modela

Table 4 The performance indices of the NN models
Tablica 4. Pokazatelji učinkovitosti NN modela

Dataset	NN-PID		ANFIS		ANN	
	Training time	MSE	Training time	MSE	Training time	MSE
20%	22s	6.273	35s	9.885	17s	5.380
40%	38s	5.231	72s	7.414	22s	3.980
60%	56s	3.866	118s	6.073	34s	2.490
80%	82s	1.533	139s	3.264	41s	0.332
100%	107s	1.854	195s	4.087	52s	0.472

The authors develop an ANN solution to control ROV motion in the MATLAB 2024a environment, using a GPU configuration with an RTX 4060 8GB graphics and 32GB RAM, which enables parallel processing to reduce calculation time. The training parameters for the NN across different motion directions are detailed in Table 3. The training process was carried out over 500 epochs to achieve optimal accuracy. Upon completion, a convergence value approaching 1 signified enhanced accuracy for the ANN. If the convergence value is inadequate, adjustments to key parameters, including the number of neurons, the choice of activation function, or the learning rate, should be made to optimize network performance. The dataset consists of 630,000 samples for each category within every information field, including *e, de*, and τ_{AFC}. Additionally, the training process requires standardizing the amount of data across the information fields and normalizing the input data using the Hyperbolic Tangent activation function, which scales the values between -1 and 1. The dataset was partitioned into three subsets: a training set (70%), a test set (15%), and a validation set (15%). The stratified division aimed to enhance the model's ability to generalize, facilitating effective adaptation to novel input values. Training outcomes for the proposed control model are illustrated in Fig. 4.

The model's performance is assessed by comparing the accuracy of predicted values to actual values during training. Shorter training durations can result in faster convergence and reduce the risk of overfitting, whereas longer training times may increase costs and require more powerful hardware. Table 4 shows that the proposed ANN model has a significantly shorter training time than a neural network online tuning (named NN-PID) [47] and the Adaptive Neuro-Fuzzy Inference System (ANFIS) [48]. As the dataset size increases from 20% to 100%, the training time for the ANN goes from 17s to 52s, while NN-PID increases from 22s to 107s and ANFIS from 35s to 195s. The performance outcome indicates that the ANN is faster and more efficient. Additionally, the MSE for the ANN is lower than that of ANFIS across all data levels, demonstrating better predictive performance. While the ANN's MSE decreases from 5.38 to 0.472 with larger datasets, it remains significantly lower than ANFIS (4.087) and NN-PID (1.854), highlighting the ANN model's effectiveness.

4.2. Results and Discussions / *Rezultati i rasprava*

4.2.1. Experiment of the ROV moving straight / *Eksperiment kretanja ROV-a po ravnoj putanji*

In Scenario 1, the ANN and AFC control methods are applied to control the ROV to follow a straight motion, starting from the reference position [0m, 0m, 0m] and moving to the desired position [20m, 10m, 20m] within a duration of 200 seconds. The first scenario is considered under calm sea conditions, with the current velocity parameters varying in the range of 0.1m/s to 0.3m/s, α_c, and in the range of [0, π/2]. The results are shown in Figs. 5 and 6. Specifically, the 3D path tracking results in Fig. 5 show that both the ANN (blue line) and AFC (red line) can control the ROV to follow the path in the scenario. Besides, Fig. 6 illustrates the control signals on the directions applying ANN and AFC controllers, allowing for a comparison of its responses.

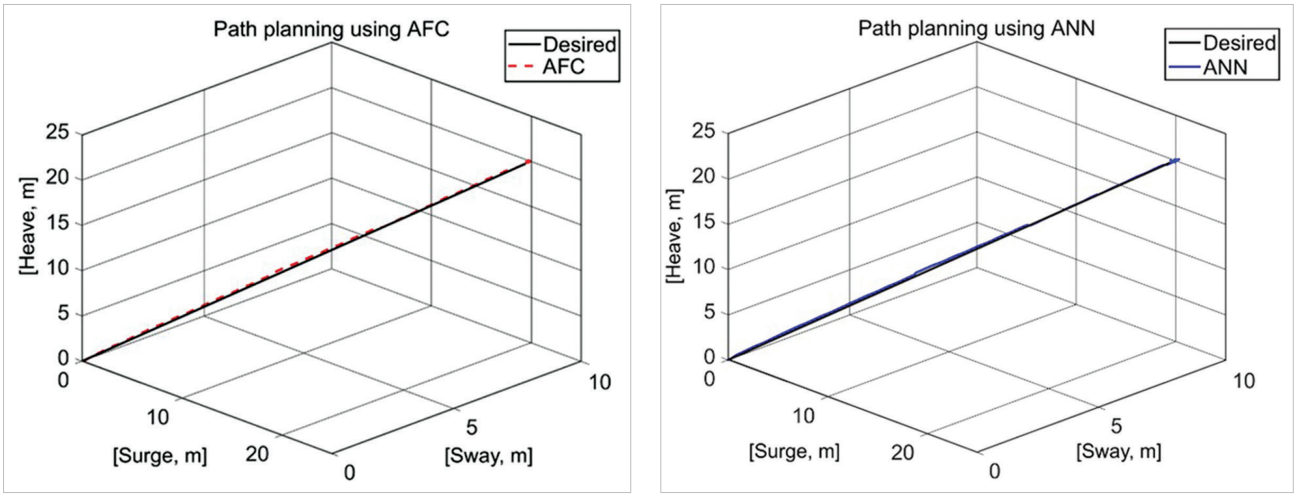

Figure 5 The ROV motion in Scenario 1
Slika 5. Kretanje ROV-a u scenariju 1

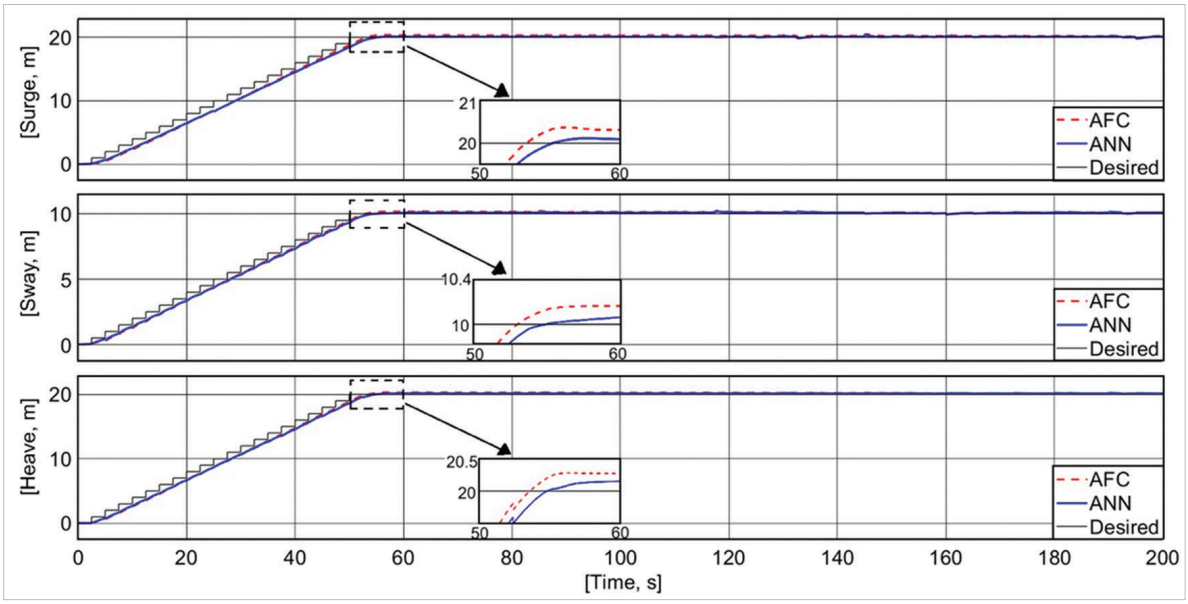

Figure 6 The results of ANN and AFC controller in Scenario 1
Slika 6. Rezultati ANN i AFC regulatora u scenariju 1

Table 5 Comparison of controller responses in Scenario 1
Tablica 5. Usporedba odziva regulatora u scenariju 1

Solution	AFC [8]			NN-PID [47]			ANFIS [48]			Proposed ANN		
	Surge	Sway	Heave	Surge	Sway	Heave	Surge	Sway	Heave	Surge	Sway	Heave
Response time (s)	53.3	53	53.6	54.8	54.8	54.7	54.4	54.1	54.7	55	55	55
Fluctuation (m)	0.62	0.32	0.32	0.56	0.3	0.23	0.56	0.31	0.23	0.55	0.28	0.22
Overshoot (%)	2.35	2.34	1.6	1.7	2.2	1.3	1.9	2.23	1.47	1.65	2.1	1.1

The response of various control solutions, including AFC, NN-PID, ANFIS, and ANN, is summarized in Table 5. The ANN has the slowest response time among the solutions, especially during a surge. The proposed controller is slower than the ANFIS controller by 0.6s, the NN-PID by 0.2s, and the AFC controller by 1.7s. However, the ANN solution shows improved response fluctuations. In the *y*-direction (sway), the ANN results are lower by 0.03m, 0.02m, and 0.04m compared to ANFIS, NN-PID, and AFC controllers, respectively. Similarly, the recorded overshoot demonstrates that the ANN shows better response results. Specifically, in the heave, the overshoot of ANN is the lowest among the approaches, as lower than 0.37%, 0.2%, and 0.5% for ANFIS, NN-PID, and AFC controllers, respectively. Therefore, although the response time is slower, other factors in evaluating the response are better, showing the capability of the ANN proposed in this study.

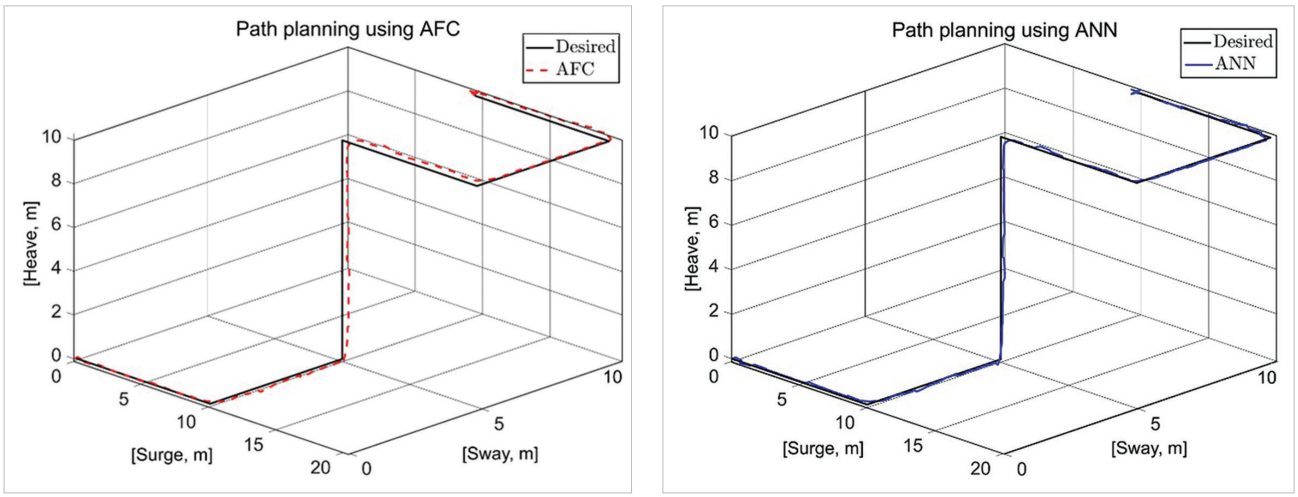

Figure 7 The path of the ROV motion in Scenario 2
Slika 7. Putanja kretanja ROV-a u scenariju 2

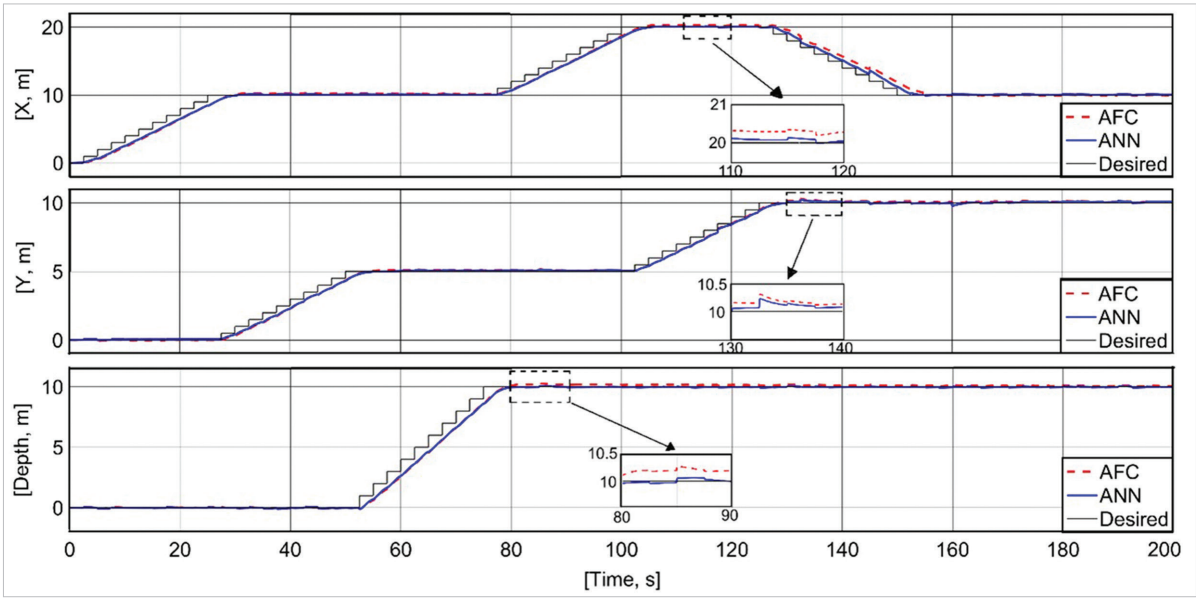

Figure 8 Response of the controllers implemented in Scenario 2
Slika 8. Odziv regulatora implementiranih u scenariju 2

Table 6 Summary of controller response comparisons in Scenario 2
Tablica 6. Sažetak usporedbi odziva regulatora u scenariju 2

Solution	AFC [8]			NN-PID [47]			ANFIS [48]			ANN		
	Surge	Sway	Heave	Surge	Sway	Heave	Surge	Sway	Heave	Surge	Sway	Heave
Response time (s)	29.5	26.6	26.7	29	27.2	29.1	30.2	27.8	29.9	30.5	28	30
Fluctuation (m)	0.44	0.45	0.28	0.21	0.42	0.18	0.23	0.43	0.17	0.21	0.41	0.15
Overshoot (%)	1.78	3.09	2.82	0.98	2.56	1.12	0.7	2.36	0.81	0.6	2.3	0.64

4.2.2. Maneuvering the ROV along its path / *Manevriranje ROV-om duž zadane putanje*

To comprehensively assess the adaptability and responsiveness of the ANN controller under realistic operating conditions for the ROV, Scenario 2 was executed, taking into account the current dynamics. The scenario involved a more intricate control path: the ROV first moved a straight path along the surge for 10m, then transitioned to a straight line in the *y*-direction for 5m, followed by a descent of 10m, culminating at the endpoint coordinates [10m, 10m, 10m]. Notably, the current velocity was elevated, exceeding 0.5m/s.

The simulation outcomes, illustrated in Figs. 7 and 8 reveal that the ANN controller (depicted by the blue line) adheres more closely to the predefined trajectory than the AFC, represented by the red line. Furthermore, Fig. 8 indicates that the control responses along each axis utilizing the ANN controller demonstrate superior performance relative to those of the AFC, highlighting the effectiveness of the ANN in managing complex control scenarios amid varying current conditions. In Scenario 2, the ROV operates in a strong current, demonstrating the advantages of the ANN controller in mitigating fluctuations and overshoots. The comparison results of the solutions are summarized in Table 6. In the surge direction, the response time of the ANN solution was recorded as 30.5s, which is 0.3s slower than ANFIS, 1.5s slower than NN-PID, and 1s slower than AFC. The ROV operates under the influence of flows with slow-changing characteristics, meaning that the accuracy of control responses is prioritized over response time. As a result, the findings from the ANN research indicate a longer response time compared to the alternative solution, which aligns with the characteristics of the control system. Additionally, the computer's performance remains within acceptable limits, with CPU usage at 10%, GPU at 5%, VRAM at 14%, and RAM at 78%.

Nevertheless, the ANN outperforms both alternatives when examining fluctuation and overshoot metrics. Specifically, the ANN's sway fluctuation is lower than that of ANFIS at 0.02m, NN-PID at 0.01m, and AFC at 0.04m. Concerning overshoot, the ANN recorded a minimum value of 0.64%, which is lower than ANFIS of 0.17%, NN-PID of 0.48%, and AFC of 2.18%. Although the ANN exhibits a longer response time, it maintains more excellent stability under identical environmental conditions compared to the ANFIS, NN-PID, and AFC, effectively addressing the concerns outlined in Remarks 1 and 2. However, the study faces limitations in training data diversity and deep feature extraction methods, which need to improve the control force accuracy in ROV operations during sudden environmental changes.

5. CONCLUSION / *Zaključak*

This paper presents a novel ANN solution designed to improve the control of ROVs over traditional control systems. The AFC framework is established to effectively address variations in input errors resulting from the nonlinearities of the operating environment. Then, the ANN is trained on various datasets, demonstrating self-learning capabilities that enable adjustments to optimize the motion control of ROVs. This adaptability is particularly relevant in complex environments where external factors, such as fluctuating water currents and turbulent conditions, pose significant challenges. Experimental

results illustrate the ANN's performance in controlling the ROV under two challenging scenarios, indicating an improvement over conventional control solutions. Additionally, there is potential for refining the training process with advanced deep-learning algorithms, which could facilitate the identification of complex patterns and features within the input data, supporting self-adjustment in environments with numerous unmeasured variables and complicating factors. To improve the dataset's quality, future studies should test under different operating conditions. Additionally, applying advanced deep learning techniques can help accurately determine the control force needed for ROV movement in unpredictable environments.

Author Contribution: X.-K.D.: Conceptualization, Methodology, writing – review and editing; Ž.K.: Review and editing; N.-H.L.P.: Numerical data calculation; V.-D.D.: Formal analysis, numerical data calculation, writing - original draft preparation; S.L.: Data curation and computing.

Conflict of interest: The authors state that there is no conflict of interest.

Acknowledgement: The authors acknowledge the facilities, and scientific and technical support from Artificial Intelligent in Transportation LAB, Ho Chi Minh City University of Transport.

REFERENCES / *Literatura*

[1] Mišković, D., Bielić, T., & Čulin, J. (2018). Impact of technology on safety as viewed by ship operators. *Transactions on Maritime Science*, *7* (1), 51-58. https://doi.org/10.7225/toms.v07.n01.005

[2] Piskur, P., Szymak, P., Flis, L., & Sznajder, J. (2020). Analysis of a fin drag force in a biomimetic underwater vehicle. *Nase More*, *67* (3), 192-198. https://doi.org/10.17818/NM/2020/3.2

[3] Rahmah, S. A., Binugroho, E. H., Dewanto, R. S., & Pramadihanto, D. (2020). Velocity control of ROV using modified integral SMC with optimization tuning based on Lyapunov analysis. *TELKOMNIKA*, *18* (3), 1505-1513. https://doi.org/10.12928/TELKOMNIKA.v18i3.14781

[4] Chen, Y., Zhang, H., Zou, W., Zhang, H., Zhou, B., & Xu, D. (2025). Dynamic modeling and learning based path tracking control for ROV-based deep-sea mining vehicle. *Expert Systems with Applications*, 262, 125612. https://doi.org/10.1016/j.eswa.2024.125612

[5] Li, Y., Zhang, J., Wang, H., Li, Y., & Sui, B. (2022). Research on heading control of USV with the lateral thruster. *Mathematical Problems in Engineering*, *2022* (1), 8359227. https://doi.org/10.1155/2022/8359227

[6] Min, F., Yang, F., Wang, G., & Ye, X. (2020). Research on the Heading Control of Underwater Vehicle under Hover Condition. *IEEE Access*, 8, 220908-220920. https://doi.org/10.1109/ACCESS.2020.3043462

[7] German-Galkin, S., & Tarnapowicz, D. (2023). Energy Optimization of a Series Hybrid Electric Ship Propulsion System. *Nase More*, *70* (1), 1-10. https://doi.org/10.17818/NM/2023/1.2

[8] Zohedi, F. N., Mohd Aras, M. S., Kasdirin, H. A., & Bahar, M. B. (2021). A new tuning approach of Single Input Fuzzy Logic Controller (SIFLC) for Remotely Operated Vehicle (ROV) depth control. *Evergreen*, *8* (3), 651-657. https://doi.org/10.5109/4491657

[9] Kitowski, Z. (2020). Communication system between the ROV and the USV's "edredon" control post. *Naše more*, *67* (2), 172-177. https://doi.org/10.17818/NM/2020/2.10

[10] Priyadarshini, L., Kundu, S., Maharana, M. K., & Ganthia, B. P. (2022). Controller design for the pitch control of an autonomous underwater vehicle. *Engineering, Technology & Applied Science Research*, *12* (4), 8967-8971. https://doi.org/10.48084/etasr.5050

[11] Desai, R. P., & Manjarekar, N. S. (2023). Pitch Channel Trajectory Tracking Control of an Autonomous Underwater Vehicle. *Lecture Notes in Electrical Engineering*, 1066, 277-288. https://doi.org/10.1007/978-981-99-4634-1_22

[12] Kuo, C. L., Pu, Y. C., & Chen, Q. A. (2022). Position Tracking of an Underwater Robot Based on Floating-Downing PI Control. *Processes*, *10* (11), 2346. https://doi.org/10.3390/pr10112346

[13] Syahab, H., Ariesta, R. C., Misbah, M. N., Zubaydi, A., Sujiatanti, S. H., Putra, W. H. A., & Setyawan, D. (2023). Structural design evaluation for Underwater Remotely Operated Vehicle (ROV), case study: Madura Straits. *Proceedings of the IOP Conference Series: Earth and Environmental Science*, 1198, 012007. https://doi.org/10.1088/1755-1315/1198/1/012007

[14] Do, V. D., & Dang, X. K. (2020). Fuzzy adaptive interactive algorithm design for marine dynamic positioning system under unexpected impacts of Vietnam Sea. *Indian Journal of Geo-Marine Sciences*, *49* (11), 1764-1771.

[15] Han, S. H., & Pham, D. A. (2024). A Study on Kinematics, Dynamics, and Fuzzy Logic Controller Design for Remotely Operated Vehicles. *Journal of Electrical Engineering and Technology*, *19* (4), 2585-2596. https://doi.org/10.1007/s42835-023-01714-6

[16] Dang, X. K., Truong, H. N., & Do, V. D. (2022). A path planning control for a vessel dynamic positioning system based on robust adaptive fuzzy strategy. *Automatika*, *63* (3), 580-592. https://doi.org/10.1080/00051144.2022.2056289

[17] Do, V. D., & Dang, X. K. (2018). Optimal control for torpedo motion based on fuzzy-PSO advantage technical. *TELKOMNIKA*, *16* (6), 2999-3007. https://doi.org/10.12928/TELKOMNIKA.v16i6.8979

[18] Liu, W., Xia, Z., Wu, L., Guo, G., Zhu, C., Zhang, Z., & Cui, L. (2023). Underwater remotely operated vehicle control system with optimized PID based on improved particle swarm optimization. *Desalination and Water Treatment*, 314, 322-329. https://doi.org/10.5004/dwt.2023.30037

[19] Tran, T. D., Do, V. D., Dang, X. K., & Mai, B. L. (2022). Improving the Control Performance of the Jacking System of Jack-Up Rig Using Self-Adaptive Fuzzy Controller Based on Particle Swarm Optimization. In *Lecture Notes of the Institute for Computer Sciences, Social-Informatics and Telecommunications Engineering, LNICST*, 444, 184-200. https://doi.org/10.1007/978-3-031-08878-0_13

[20] Ronghua, M., Xinhao, C., Zhengjia, W., & Du, X. (2024). Improved ant colony optimization for safe path planning of AUV. *Heliyon*, *10* (7), e27753. https://doi.org/10.1016/j.heliyon.2024.e27753

[21] Hasan, M. W., & Abbas, N. H. (2023). An adaptive neural network with nonlinear FOPID design of underwater robotic vehicle in the presence of disturbances, uncertainty, and obstacles. *Ocean Engineering*, 279, 114451. https://doi.org/10.1016/j.oceaneng.2023.114451

[22] Setyawan, A., & Mashoedah. (2021). Remotely Operated Underwater Vehicle (ROV) stabilization with Artificial Neural Networks (ANN). *Journal of Physics: Conference Series*, 1833, 012068. https://doi.org/10.1088/1742-6596/1833/1/012068

[23] Liu, H., Meng, B. & Tian, X. (2022). Finite-Time Prescribed Performance Trajectory Tracking Control for Underactuated Autonomous Underwater Vehicles Based on a Tan-Type Barrier Lyapunov Function. *IEEE Access*, 10, 53664-53675. https://doi.org/10.1109/ACCESS.2022.3175854

[24] Liu, H., Yuan, J., Ren, Q., Li, M., Qi, Z., & Deng, X. (2025). Remotely operated vehicle (ROV) underwater vision-based micro-crack inspection for concrete dams using a customizable CNN framework. *Automation in Construction*, 173, 106102. https://doi.org/10.1016/j.autcon.2025.106102

[25] Chtouki, I., Patrice, W. I. R. A., Malika, Z. A. Z. I., Chakir, H. E., Motahhir, S. A. A. D., & Choukri, K. (2025). Maximum Power Point tracking implementation based on self-learning adaptive GA-Neural controller for standalone PV applications. *Results in Engineering*, 26, 104587. https://doi.org/10.1016/j.rineng.2025.104587

[26] Zohedi, F. N., Aras, M. S. M., Kasdirin, H. A., & Nordin, N. B. (2022). New lambda tuning approach of single input fuzzy logic using gradient descent algorithm and particle swarm optimization. *Indonesian Journal of Electrical Engineering and Computer Science*, *25* (3), 1344-1355. https://doi.org/10.11591/ijeecs.v25.i3.pp1344-1355

[27] Yang, M., Sheng, Z., Yin, G., & Wang, H. (2022). A recurrent neural network based fuzzy sliding mode control for 4-DOF ROV movements. *Ocean Engineering*, 256, 111509. https://doi.org/10.1016/j.oceaneng.2022.111509

[28] Rafia, H., Ouadi, H., & El Bhiri, B. (2024). Ann-pi controller for the grid-side converters in wind energy conversions systems under voltage dips. *IFAC-PapersOnLine*, *58* (13), 575-580. https://doi.org/10.1016/j.ifacol.2024.07.544

[29] Zarkasi, A., Satria, H., Primanita, A., Abdurahman, A., Afifah, N., & Sutarno, S. (2024). A new system for underwater vehicle balancing control based on weightless neural network and fuzzy logic methods. *IAES International Journal of Artificial Intelligence (IJ-AI)*, *13* (3), 2870-2882. https://doi.org/10.11591/ijai.v13.i3.pp2870-2882

[30] Sang, I. C., & Norris, W. R. (2023). An Autonomous Underwater Vehicle Simulation with Fuzzy Sensor Fusion for Pipeline Inspection. *IEEE Sensors Journal*, *23* (8), 8941.8951. https://doi.org/10.1109/JSEN.2023.3250721

[31] Ben Jabeur, C., & Seddik, H. (2022). Application of PD and Fuzzy Controllers for an UROV. In *2022 IEEE Information Technologies and Smart Industrial Systems, ITSIS 2022*, 1-5. https://doi.org/10.1109/ITSIS56166.2022.10118395

[32] Fossen, T. I. (2011). *Handbook of Marine Craft Hydrodynamics and Motion Control*. John Wiley and Sons. https://doi.org/10.1002/9781119994138

[33] Dang, X. K., Do, V. D., Do, V. T., & Ho, L. A. H. (2021). Enhancing the Control Performance of Automatic Voltage Regulator for Marine Synchronous Generator by Using Interactive Adaptive Fuzzy Algorithm. *Lecture Notes of the Institute for Computer Sciences, Social Informatics and Telecommunications Engineering*, 379, 379-392. https://doi.org/10.1007/978-3-030-77424-0_31

[34] Joseph, S. B., Dada, E. G., Abidemi, A., Oyewola, D. O., & Khammas, B. M. (2022). Metaheuristic algorithms for PID controller parameters tuning: review, approaches and open problems. *Heliyon*, *8* (5), e09399. https://doi.org/10.1016/j.heliyon.2022.e09399

[35] Do, V. D., Dang, X. K., Tran, T. D., & Pham, T. D. A. (2022). Jacking and Energy Consumption Control over Network for Jack-Up Rig: Simulation and Experiment. *Polish Maritime Research*, *29* (3), 89-98. https://doi.org/10.2478/pomr-2022-0029

[36] Nguyen, X. P., Dang, X. K., Do, V. D., Corchado, J. M., & Truong, H. N. (2023). Robust Adaptive Fuzzy-Free Fault-Tolerant Path Planning Control for a Semi-Submersible Platform Dynamic Positioning System With Actuator Constraints. *IEEE Transactions on Intelligent Transportation Systems*, *24* (11), 12701-12715. https://doi.org/10.1109/TITS.2023.3297252

[37] Lodi, K. A., Beig, A. R., Al Jaafari, K. A., & Aung, Z. (2024). Ann-based improved direct torque control of open-end winding induction motor. *IEEE Transactions on Industrial Electronics*, *71* (10), 12030-12040. https://doi.org/10.1109/TIE.2024.3357865

[38] Laabid, Z., Moumen, A., Mansouri, K., & Siadat, A. (2023). Numerical study of the speed's response of the various intelligent models using the tansig, logsig and purelin activation functions in different layers of artificial neural network. *IAES International Journal of Artificial Intelligence*, *12* (1), 155-161. https://doi.org/10.11591/ijai.v12.i1.pp155-161

[39] Pham, T. A., Dang, X. K., Koboevic, Z., Do V. D., & Pham, T. D. A. (2024). Maritime Data Mining for Marine Safety Based on Deep Learning: Southern Vietnam Case Study. *Nase More*, *71* (1), 21-29. https://doi.org/10.17818/NM/2024/1.4

[40] Yan, H., Chen, H., Zhang, W., Shuai, M., & Huang, B. (2024). Strength prediction and optimization for microwave sintering of large-dimension lithium hydride ceramics: GA-BP-ANN modeling. *Nuclear Materials and Energy*, 41, 101801. https://doi.org/10.1016/j.nme.2024.101801

[41] Lekshmi, S., & PS, L. P. (2024). Hierarchical predictive optimal control for range extension of EV with ANN based torque control for IPMSM drives. *E-Prime-Advances in Electrical Engineering, Electronics and Energy*, 10, 100772. https://doi.org/10.1016/j.prime.2024.100772

[42] Mišković, D., Ivče, R., Hess, M., & Koboević, Ž. (2022). The Influence of Shipboard Safety Factors on Quality of Safety Supervision: Croatian Seafarer's Attitudes. *Journal of Marine Science and Engineering*, *10* (9), 1-13. https://doi.org/10.3390/jmse10091265

[43] Husain, S., Kadirbay, B., Jarndal, A., & Hashmi, M. (2023). Comprehensive Investigation of ANN Algorithms Implemented in MATLAB, Python, and R for Small-Signal Behavioral Modeling of GaN HEMTs. *IEEE Journal of the Electron Devices Society*, 11, 559-572. https://doi.org/10.1109/JEDS.2023.3324084

[44] Dampfhoffer, M., Mesquida, T., Valentian, A., & Anghel, L. (2024). Backpropagation-Based Learning Techniques for Deep Spiking Neural Networks: A Survey. *IEEE Transactions on Neural Networks and Learning Systems*, *35* (9), 11906-11921. https://doi.org/10.1109/TNNLS.2023.3263008

[45] Huzir, S. M. H. M., Al-Hadi, A. H. I. H., Yusoff, Z. M., Ismail, N., & Taib, M. N. (2024). Accurate Agarwood Oil Quality Determination: A Breakthrough with Artificial Neural Networks and the Levenberg-Marquardt Algorithm. *IEEE Access*, 12, 50389-50403. https://doi.org/10.1109/ACCESS.2024.3381627

[46] Eslami, M., Chin, C. S., & Nobakhti, A. (2019). Robust modeling, sliding-mode controller, and simulation of an underactuated ROV under parametric uncertainties and disturbances. *Journal of marine science and application*, 18, 213-227. https://doi.org/10.1007/s11804-018-0037-1

[47] Hernández-Alvarado, R., García-Valdovinos, L. G., Salgado-Jiménez, T., Gómez-Espinosa, A., & Fonseca-Navarro, F. (2016). Neural network-based self-tuning PID control for underwater vehicles. *Sensors (Switzerland)*, *16* (9), 1429. https://doi.org/10.3390/s16091429

[48] Trslić, P., Omerdic, E., Dooly, G., & Toal, D. (2020). Neuro-fuzzy dynamic position prediction for autonomous work-class ROV docking. *Sensors*, *20* (3), 693. https://doi.org/10.3390/s20030693